

OLD DOMINION UNIVERSITY RESEARCH FOUNDATION

184-30274

DEPARTMENT OF PHYSICS
SCHOOL OF SCIENCES AND HEALTH PROFESSIONS
OLD DOMINION UNIVERSITY
NORFOLK, VIRGINIA

Technical Report PTR 84-4

THEORETICAL STUDIES OF SOLAR-PUMPED LASERS

By

Wynford L. Harries, Principal Investigator

and

Zeng-Shevan Fong, Graduate Research Assistant

Progress Report

For the period January 15 to July 15, 1984

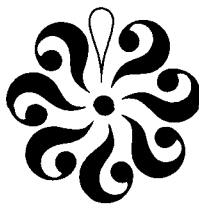
Prepared for the
National Aeronautics and Space Administration
Langley Research Center
Hampton, Virginia 23665

Under

Research Grant NSG 1568

W. E. Meador, Technical Monitor
Space Systems Division

July 1984



DEPARTMENT OF PHYSICS
SCHOOL OF SCIENCES AND HEALTH PROFESSIONS
OLD DOMINION UNIVERSITY
NORFOLK, VIRGINIA

Technical Report PTR 84-4

THEORETICAL STUDIES OF SOLAR-PUMPED LASERS

By

Wynford L. Harries, Principal Investigator

and

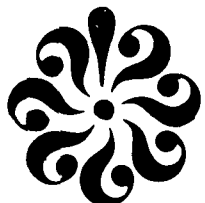
Zeng-Shevan Fong, Graduate Research Assistant

Progress Report
For the period January 15 to July 15, 1984

Prepared for the
National Aeronautics and Space Administration
Langley Research Center
Hampton, Virginia 23665

Under
Research Grant NSG 1568
W. E. Meador, Technical Monitor
Space Systems Division

Submitted by the
Old Dominion University Research Foundation
P.O. Box 6369
Norfolk, Virginia 23508



July 1984

TABLE OF CONTENTS

	<u>Page</u>
SUMMARY.....	1
1. INTRODUCTION.....	1
2. PHYSICAL MECHANISMS IN THE LASER.....	3
2.1 Absorption of Radiation.....	3
2.2 Heating of the Medium.....	5
2.3 Filling of the Lower Laser Level.....	7
2.4 Diffusion Losses.....	7
2.5 The Kinetic Equations.....	8
3. TIME VARYING SOLUTIONS.....	13
4. STEADY STATE SOLUTIONS.....	13
4.1 Power Output.....	16
4.2 Efficiency.....	21
CONCLUSIONS.....	21
ACKNOWLEDGEMENTS.....	22
REFERENCES.....	23
APPENDIX: Diffusion of CO ₂ When Mixed with He and Ar.....	24

LIST OF TABLES

<u>Table</u>		<u>Page</u>
1	Rate Coefficients for CO ₂ at 360°K.....	9

LIST OF FIGURES

<u>Figure</u>		<u>Page</u>
1	Flow diagram for CO ₂ black body laser.....	4
2	Time behavior of black body pumped laser. The pumping signal was assumed proportional to $\sin^2(\pi t/2 \times 10^{-4})$ up to 100μs, then became constant. The middle diagram shows N _u , N ₁ , and (N _u -N ₁)x10. The lower diagram shows the 10.6μ photon density.....	14

TABLE OF CONTENTS - (Continued)

LIST OF FIGURES - (Continued)

<u>Figure</u>		<u>Page</u>
3	Power output of black body pumped laser vs total pressure for various black body temperatures. The gases were CO ₂ -16%, He-4%, Ar-80°. The wall temperature was 340K.....	17
4	Power output vs black body temperature; Total pressure 7 torr, 16% CO ₂ , 4% He 80%, Ar, wall temperature 340K.....	18
5	Efficiency (as defined by equation 29) of the black body pumped laser vs total pressure P for various black body temperatures. The gases were CO ₂ 16%, He 4% and Ar 80°.....	19
6	Plot of power output vs gas temperature; total pressure 7 torr, 16% CO ₂ , 4% He, 80% Ar, black body temperature 1450K.....	20

THEORETICAL STUDIES OF SOLAR-PUMPED LASERS

By

Wynford L. Harries¹ and Zeng-Shevan Fong²

SUMMARY

A method of pumping a CO₂ laser by a hot cavity has been demonstrated (ref. 1). The cavity, heated by solar radiation, should increase the efficiency of solar pumped lasers used for energy conversion. Kinetic modeling is used to examine the behavior of such a CO₂ laser. The kinetic equations are solved numerically vs. time and, in addition, steady state solutions are obtained analytically. The effect of gas heating filling the lower laser level is included. The output power and laser efficiency are obtained as functions of black body temperature and gas ratios (CO₂-He-Ar) and pressures. The values are compared with experimental results.

1. INTRODUCTION

The possibility of using solar collectors on orbiting space vehicles and transmitting the energy to earth via laser beams has been discussed already (refs. 2, 3, 4). A critical factor for energy conversion is the laser efficiency. One suggestion for increasing the efficiency is to heat a black body cavity by solar radiation and then let the cavity pump the laser, according to the Planck radiation law. If the laser medium absorbed a narrow bandwidth from the spectrum then the black body cavity would immediately refill any "hole" in the distribution. The pumping radiation is thus

¹Eminent Professor, Department of Physics, Old Dominion University, Norfolk, Virginia 23508.

²Graduate Research Assistant, Department of Physics, Old Dominion University, Norfolk, Virginia 23508.

replenished and the potential efficiency should be much higher than if the laser is pumped directly.

It is the purpose of this paper to examine the kinetics of a black body pumped laser. In addition to directly pumped CO₂ lasers, there are schemes whereby N₂ is pumped and the energy transferred to CO₂, but these are not considered here. The direct CO₂ lasers usually have He and Ar as additives which perform the functions of deexcitation of the lower level and heat conduction; these are included.

The physical mechanisms of the laser are discussed in Section 2. For the first time to our knowledge the effect of gas heating, which serves to fill the lower laser level and inhibit lasing, is included. The temperature rise is calculated, and an estimate of the effect of filling the lower laser level from Boltzmann statistics is made.

In Section 3, time varying solutions of the kinetic equations show the behavior of the upper and lower laser level densities, and also the photon density and output power vs. time. The solutions show that steady state conditions can be achieved.

Analytical solutions are obtained for the steady state in Section 4. The steady state output power is shown as a function of black body temperature and gas constituent pressures. Estimates of the laser efficiency as a function of the variables are also given.

Throughout the discussion it is assumed that the laser tube of 0.4 cm radius has a length of 50 cm heated in an oven at 1000-1500 K and contains CO₂+He+Ar at total pressures of 1 to 12 torr in varying ratios. The radiation from the oven is passed through nitrogen which is transparent to it and enters the laser tube. The purpose of the nitrogen, which is flowed, is to cool the laser medium. The measured exit temperature of the nitrogen was 340 K (ref. 1), and this was assumed to be the wall temperature. The gas

temperature is slightly higher than this and is discussed in Section 2.2. The above numbers correspond to experimental conditions in reference 1.

2. PHYSICAL MECHANISMS IN THE LASER

A flow diagram of the processes occurring during lasing is shown in figure 1.

2.1 Absorption of Radiation

The black body radiation is absorbed at 4.256μ over a bandwidth of 0.1μ . The radiation flux per unit length entering the laser tube of radius r is $E(\lambda) d\lambda 2\pi r$ when $E(\lambda)$ is determined by Planck's radiation formula and $d\lambda$ is 0.1μ . The fraction absorbed depends on σ_a , the absorption cross section. The latter can be calculated: $\sigma_a = \lambda^2 A / 4\pi^2 \Delta\nu$, where $A = 424.6$ is the Einstein coefficient for the transition $(000)\rightarrow(001)$, $\lambda = 10.6\mu$, $\Delta\lambda = 0.1\mu$ and $\sigma_a = 1.2 \times 10^{-18} \text{ cm}^2$. However, a measured value of the absorption length is $1.56 \times 10^{-3} \text{ cm}$ at 1 atmosphere (ref. 5), which yields $\sigma_a = 2.41 \times 10^{-17} \text{ cm}$. Both values were tried.

Two possibilities exist for the calculation of the fraction absorbed. If the absorption is small, then the fraction absorbed per unit volume can be expressed approximately as

$$F_1 = 2 (1 - \exp(-(C_{O_2}) \sigma_a 2r)) / r \quad (1)$$

where the radiation is assumed to cross a distance $2r$ and the amount per unit length is proportional to $2\pi r$ and per unit volume, $2\pi r / \pi r^2$. If the pressure increases, however, the absorption will take place at the outer edges of the tube. The excited species can, however, diffuse to the center in a time t where $t \approx r^2/D$ and D is the diffusion coefficient. Assuming a mean free path of $2.9 \times 10^{-3} \text{ cm}$ at 1 torr, a total gas pressure of 1 torr

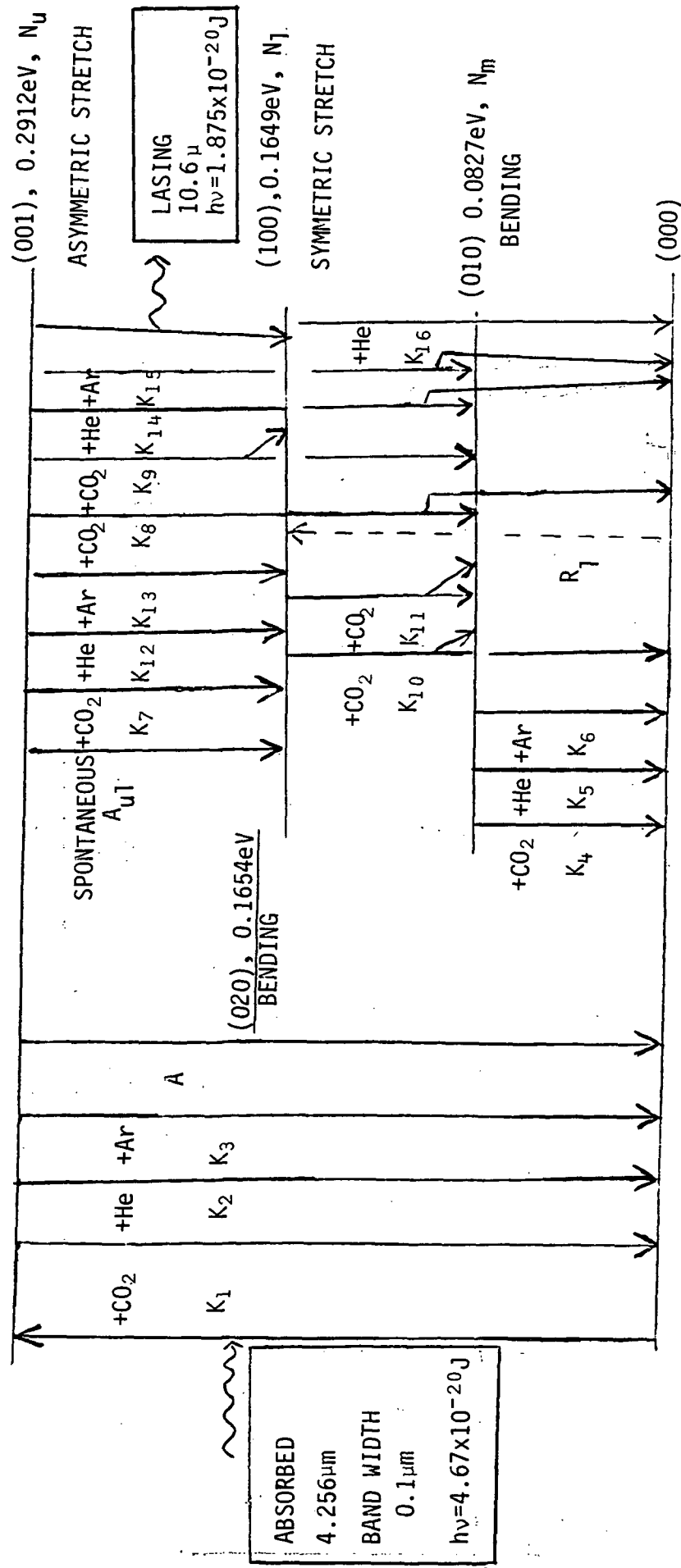


Figure 1. Flow Diagram for CO_2 Black Body Laser

(ref. 6) and a temperature of 340° , then $t \approx 3$ ms, a time comparable with other rates. Neglecting diffusion, a second estimate is obtained by assuming the radiation is absorbed at the center of the tube between a depth x_1 and x_2 . Then the fraction F absorbed per unit volume is

$$F_2 = (\exp(-(CO_2)\sigma_a x_1) - \exp(-(CO_2)\sigma_a x_2))/(x_2 - x_1) \quad (2)$$

where here $x_1 = 0.35$, $x_2 = 0.45$ cm. The effect of the outer layer of gas shielding the center of the tube at high pressures is now included, but a one dimensional, not cylindrical, geometry is assumed.

A number of computer runs were made using F_2 , however, the results did not agree with the experiment (ref. 1). The computer results showed a sharp cutoff of power at a few torr and, accordingly, the coefficient F_1 was used for the following calculations.

The number of absorption events per unit volume is then

$$S = \frac{E(\lambda)d\lambda}{hv} F_1 = 5.76 \times 10^{19} F_1 / (\exp(3381/T_b) - 1) \quad (3)$$

where T_b is the black body temperature, which gives the number of $CO_2(000)$ molecules raised to the upper laser level $CO_2(001)$ per cc per second.

2.2 Heating of the Medium

Experimentally it was realized that unless a nitrogen coolant was flowed past the laser tube, that lasing ceased (ref. 1). The implication was that the medium became heated causing the lower level to be filled. A rough estimate of the increase in temperature, and its effect on the density of the lower level follows.

As the efficiency of the laser would probably not be greater than a few percent, it is assumed that all the radiation absorbed goes into heating the gases. The rate at which heat energy enters a unit volume, dQ/dt , increases with the pressure of CO_2 which is included in $F_{1,2}$.

$$dQ/dt = E(\lambda) d\lambda \cdot F_1 / 4.2 \text{ Cals cm}^{-3} \text{s}^{-1} \quad (4)$$

The heat conduction K of a mixture of gases CO_2 , He, Ar depends on the gas ratios and the absolute temperature (ref. 3). It is independent of gas pressure.

$$K = 3.27 \times 10^{-4} \text{ S } \sqrt{T/273} \quad (5)$$

where

$$S = \left(\frac{1 + 0.71 \text{ CO}_2/\text{He} + 0.32 \text{ Ar/He}}{1 + 4.55 \text{ CO}_2/\text{He} + 2.67 \text{ Ar/He}} \right) \quad (6)$$

It is assumed that the heat is conducted over an effective area A through an effective distance d to the wall at a temperature T_w . As the conduction is proportional to \sqrt{T} , the conduction equation yields that the temperature in the center of the gas T_g is:

$$T_g \approx (T_w + 1.8 \times 10^4 \cdot (dQ/dt)/(S \cdot A/d))^{2/3} \quad (7)$$

The expression is approximate as a one dimensional geometry is assumed. For example, with $T_w = 340 \text{ K}$,⁽¹⁾ a black body temperature of 1500 K, a total pressure of 10 torr (CO_2 20%, He 20%, Ar 60%), tube radius 0.4 cm, then T_g approaches 360 K.

2.3 Filling of the Lower Laser Level

The lower laser level which has a density N_1 of $\text{CO}_2(100)$ atoms, will be filled according to Boltzmann statistics which depend on T_g . However competing against this will be the depletion processes due to collisions. To include the temperature effects they must be expressed as a rate of production of N_1 vs. time. It is assumed that CO_2 molecules in the tail of the energy distribution, which have energies greater than $E_1 = 0.1649\text{eV}$, the energy of the lower laser level, can collide with the rest of the CO_2 population with a finite probability of producing $\text{CO}_2(100)$. The density of molecules with sufficient energy is $(\text{CO}_2) \exp(-E_1/kT)$ and the rate of production R_1 from this process is:

$$R_1 = (\text{CO}_2) (\text{CO}_2 \cdot \exp(-E_1/kT_g)) \overline{\sigma v} \quad (8)$$

Here k is Boltzmann's constant, σ is the cross section for the reaction, v the particle velocity. R_1 increases as T_g increases.

2.4 Diffusion Losses

At low pressures losses of particles by diffusion to the tube walls may be important. We assume that the diffusion loss time of CO_2 molecules, τ_D obeys (ref. 7):

$$\tau_D = (r/2.405)^2/D \quad (9)$$

where D is the diffusion coefficient for CO_2 in a mixture of CO_2 , He and Ar, (Appendix I) and the 2.405 corresponds to losses in an infinitely long cyl-

inder. The quantity γ is the probability of deexcitation at the wall and is somewhere between 0.2 and 1. The diffusion losses apply equally to all excited levels of CO_2 .

2.5 The Kinetic Equations

The CO_2 laser (Fig. 1) is a four level system. The absorbed photon raises the $\text{CO}_2(000)$ level to the upper laser level $\text{CO}_2(001)$ the asymmetric stretching mode at 0.2912 eV above ground. Lasing at 10.6μ occurs by a transition between the (001) and (100) levels, the latter a symmetric stretching mode at 0.1649 eV above ground.

The upper laser level of density N_u is depopulated by collisions with CO_2 , He, Ar (rate constants K_1 , K_2 , K_3) to the ground level, and by spontaneous emission (Einstein coefficient A). Transitions can also occur to the lower laser level (100) (K_7 , K_9 , K_{12} , K_{13} , and the spontaneous coefficient A_{u1}) and the (010) level (K_8 , K_9 , K_{14} , K_{15}).

The (100) level (density N_1) has a (020) bending mode which is, 0.0005 eV higher in energy. The conversion $(020) \rightarrow (100)$ is very rapid, and the two are lumped together here.

The lower laser level is filled by collisions from the upper level (K_7 , K_9 , K_{12} , K_{13}) and by the spontaneous emission A_{u1} . It is also filled during lasing by stimulated transitions of rate constant Γ . The lower level is depleted by collisions with CO_2 (K_{10} , K_{11}) and with He (K_{16}), (no data on Ar was available), and the transitions end either on the (010) level or the (000). However, at high gas temperatures, the lower laser level will be filled at a rate R_1 .

The (010) level of density N_m is in turn depleted by collision with CO_2 , He, Ar (K_4 , K_5 , K_6). The reactions are given in more detail in Table 1,

Table 1. Rate Coefficients for CO_2 at 360°K

Reaction	Coeff.	Ref. 8 EXPT.	Ref. 9 CALCULATED	Ref. 10 EXPT.	Ref. 11 EXPT.	Ref. 12	Value Assumed
$\text{CO}_2(001) + \text{CO}_2(000) + \text{CO}_2(000)$	K_1		$+N_2 4.2 \times 10^{-13}$	1.33×10^{-14}		1.33×10^{-14}	
+He+	+He	K_2	$+CO_2 2.35 \times 10^{-13}$			$? 3.6 \times 10^{-15}$	
+Ar+	+Ar	K_3		4.73×10^{-16}	4.2×10^{-15}	$? 2.5 \times 10^{-15}$	
$\text{CO}_2(001) + \text{CO}_2(100) + \text{CO}_2(000)$	K_7					4.2×10^{-15}	
+He	+He	K_{12}				$? 2.48 \times 10^{-15}$	
+Ar	+Ar	K_{13}				$? 1.87 \times 10^{-15}$	
$\text{CO}_2(001) + \text{CO}_2(010) + \text{CO}_2(000)$	K_8	5.5×10^{-15}	7.13×10^{-19}	6.3×10^{-18}	6×10^{-15}	$6.10^{-15}, 6.3 \times 10^{-18}$	
+He	+He	K_{14}	2×10^{-15}			1.08×10^{-15}	
+Ar	+Ar	K_{15}				1.03×10^{-15}	
$\text{CO}_2(001) + \text{CO}_2(100) + \text{CO}_2(010)$	K_9		9.72×10^{-15}			9.72×10^{-15}	
$\text{CO}_2(100) + \text{CO}_2(010) + \text{CO}_2(000)$	K_{10}			4.64×10^{-18}		4.6×10^{-18}	
$\text{CO}_2(100) + \text{CO}_2(010) + \text{CO}_2(010)$	K_{11}			2.53×10^{-14}		2.53×10^{-14}	
$\text{CO}_2(010) + \text{CO}_2(000) + \text{CO}_2(000)$	K_4	8×10^{-15}	8.29×10^{-15}	6.67×10^{-15}	1×10^{-14}	8×10^{-15}	
+He	+He	K_5	1.5×10^{-13}		2×10^{-13}	1.39×10^{-13}	
+Ar	+Ar	K_6			2×10^{-15}	2×10^{-15}	
$\text{CO}_2(100) + \text{He} + \text{CO}_2(010, 000) + \text{He}$			—				
+Ar+CO ₂ (010, 000)			—				
Spontaneous A (001)+000	A					424.6	
A (001)+(100)	A_{u1}					0.186	
$\text{CO}_2(100) + \text{He} + \text{CO}_2(000) + \text{He}$	K_{16}	1.025×10^{-13}				1.025×10^{-13}	
+Ar+CO ₂ (000)+Ar		—					

with values from four different sources. In the column under reference 9, the values are calculated from the expression

$$\ln K = A + BT^{-1/3} + CT^{-2/3} \quad (10)$$

where the constants A, B, C, are given for the different reactions. The values may not be accurate when extrapolated to 360K. References 8, 10 and 11 give experimental values.

The unknown quantities are then assumed to be N_u , N_1 , N_m and N the 10.6μ photon density. In the following equations, the quantities in parenthesis (CO_2) etc. are the densities of the species. The rate equations for the four species are:

$$\frac{dN_u}{dt} = S - N_u \left[(K_1 + K_7 + K_8 + K_9)(\text{CO}_2) + (K_2 + K_{12} + K_{14})(\text{He}) + (K_3 + K_{13} + K_{15})\text{Ar} \right] - N_u(A + A_{u1}) - r - \frac{N_u}{\tau_D} \quad (11)$$

$$\frac{dN_1}{dt} = r + N_u A_{u1} + N_u \left[(K_7 + K_9)(\text{CO}_2) + K_{12}(\text{He}) + K_{13}(\text{Ar}) \right] - N_1 \left[(K_{10} + K_{11})(\text{CO}_2) + K_{16}(\text{He}) \right] - \frac{N_e}{\tau_D} + R_1 \quad (12)$$

$$\frac{dN_m}{dt} = N_1 (K_{10} + 2K_{11})(\text{CO}_2) + N_u \left[(K_8 + K_9)(\text{CO}_2) + K_{14}(\text{He}) + K_{15}(\text{Ar}) \right] - N_m \left[K_4(\text{CO}_2) + K_5(\text{He}) + K_6(\text{Ar}) \right] - \frac{N_m}{\tau_D} \quad (13)$$

$$\frac{dN}{dt} = \Gamma + G A_{u1} N_u - \frac{N}{\tau_c} \quad (14)$$

The stimulated emission rate Γ is given by:

$$\Gamma = N \sigma_e c [N_u - N_l] \quad (15)$$

and is proportional to the stimulated emission cross section σ_e whose value was calculated: $\sigma_e = \lambda_e^4 A_{u1} / 4\pi^2 c \Delta\lambda_e$, where $\lambda_e = 10.6\mu$, $A_{u1} = 0.186$ and $\Delta\lambda_e$ was taken as the bandwidth from Doppler Broadening. Here c is the velocity of light. Assuming a gas temperature of 360° , then $\Delta\lambda_e = 0.217\text{\AA}$ and $\sigma_e = 9.14 \times 10^{-17} \text{cm}^2$.

In equation 15 the quantity G is a geometrical factor which takes into account that the spontaneous emission is isotropic; $G = 2r^2/L^2$ where r and L are the radius and length of the laser. The quantity τ_c is the containment time for photons, $\tau_c = -2L/c \ln(r_1 r_2)$ where $r_1 = 0.99$, $r_2 = 0.95$ are the reflectivities of the laser mirrors.

The equations can be simplified by noting that N_u , N_l , $N_m \ll (\text{CO}_2)$, and that (CO_2) can be regarded as constant. Then the following constants can be defined:

$$a_1 = [(K_1 + K_7 + K_8 + K_9)(\text{CO}_2) + (K_2 + K_{12} + K_{14})(\text{He}) + (K_3 + K_{13} + K_{15})(\text{Ar}) \\ + A + A_{u1} + \frac{1}{\tau_D}]$$

$$a_2 = [(K_{10} + K_{11})(CO_2) + K_{16}(He) + \frac{1}{\tau_D}]$$

$$A' = [(K_7 + K_9)(CO_2) + K_{12}(He) + K_{13}(Ar) + A_{u1}]$$

$$a_3 = [K_4(CO_2) + K_5(He) + K_6(Ar)]$$

$$a_4 = [(K_{10} + 2K_{11})(CO_2)]$$

$$a_5 = [(K_8 + K_9)(CO_2) + K_{14}(He) + K_{15}(Ar)]$$

Then equations 11 through 14 can be reduced to

$$\frac{dN_u}{dt} = S - a_1 N_u - \Gamma \quad (16)$$

$$\frac{dN_1}{dt} = \Gamma + A' N_u - a_2 N_1 + R_1 \quad (17)$$

$$\frac{dN_m}{dt} = a_5 N_u + a_4 N_1 - a_3 N_m \quad (18)$$

$$\frac{dN}{dt} = \Gamma + G A_{u1} N_u - N / \tau_c \quad (19)$$

3. TIME VARYING SOLUTIONS

Computer graphic solutions of equations 15 through 19 are shown in Figure 2. It was assumed for convenience that the pumping signal from the black body rose from zero to full value in a time of 100 μ s, and that the signal was proportional to $\sin^2 2\pi (t/10^{-4})$ (where t is the time in seconds) up to 100 μ s; thereafter it was constant. The pumping signal is shown in the upper curve.

In the second plot, N_u , N_l and $(N_u - N_l) \times 10$ are plotted. The densities of the upper and lower laser levels increase with time, but at first, when the signal is small, $N_l > N_u$. (This can be seen on amplified plots). However, N_u overtakes N_l at 28 μ s, and the signal $(N_u - N_l)$ starts to grow. It increases with time until threshold at $t = 53 \mu$ s. Then N_u falls and N_l rises, and the inversion $(N_u - N_l)$ falls. At the same time the photon density N increases sharply and then falls to zero as the inversion falls. The upper level is then increased again until a second light pulse appears and so on. This behavior is characteristic of kinetic equations similar to these, where σ_e is small; if σ_e is much larger these violet oscillations are smoothed out.

The inversion quickly assumes a constant value, and at 135 μ s the value of the photon density N also becomes constant. This implies that continuous lasing is possible.

4. STEADY STATE SOLUTIONS

As they stand, equations 16 through 19 are nonlinear. In the steady state, however, the stimulated emission rate far exceeds the spontaneous rate, and in equation 19, $\Gamma \gg G A_{ul} N_u$ or:

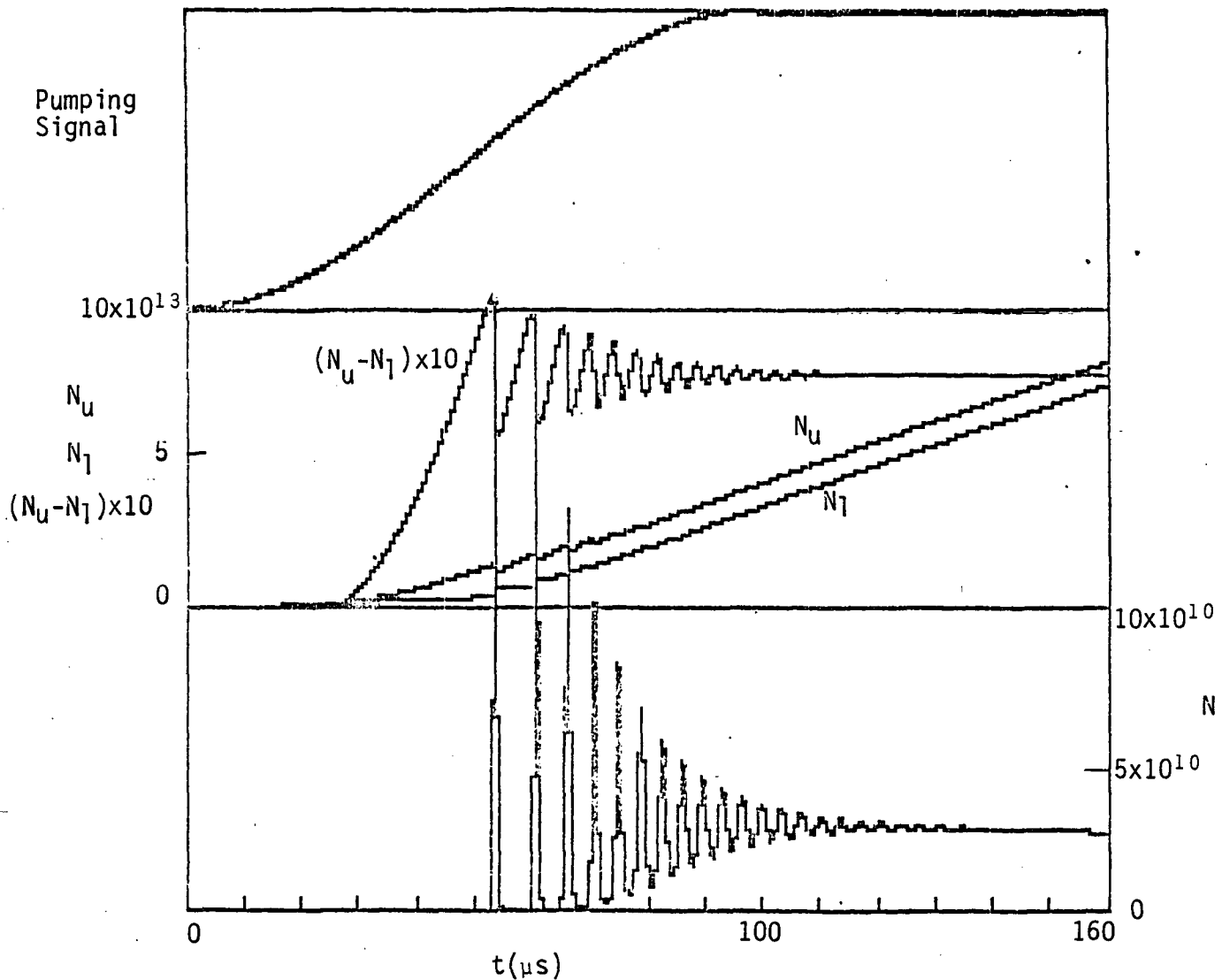


Figure 2. Time behavior of black body pumped laser. The pumping signal was assumed proportional to $\sin^2(\pi t/2 \times 10^{-4})$ up to $100\mu s$, then became constant. The middle diagram shows N_u , N_l and $(N_u - N_l) \times 10$. The lower diagram shows the 10.6μ photon.

$$\Gamma \approx N/\tau_c \quad (20)$$

and from 15 and 19

$$N_u - N_1 \approx \frac{1}{\sigma_e c \tau_c} = \text{const} \quad (21)$$

The constancy of the inversion $N_u - N_1$ is evident in Figure 2, and the value is given by equation 21. Replacing Γ in equations 16 through 19 by N/τ_c the solutions are

$$N_u = \frac{s + R_1 + a_2/\tau_c \sigma_e c}{a_1 + a_2 - A'} \quad (22)$$

$$N_1 = N_u - \frac{1}{\tau_c \sigma_e c} \quad (23)$$

$$N_m = \frac{a_5 N_u + a_4 N_1}{a_3} \quad (24)$$

$$N = \tau_e s \left[1 - \frac{a_1}{a_1 + a_2 - A'} \right] - \left[\frac{a_1 a_2}{\sigma_e c (a_1 + a_2 - A')} \right] - \left[\frac{\tau_c R_1 a_1}{a_1 + a_2 - A'} \right] \quad (25)$$

The effect of gas temperature is included in R_1 and as R_1 increases the value of N falls.

The value of N from equation 25 agrees with the value, late in time, from the time varying computer solutions.

4.1 Steady State Power Output

The evaluation of N enables the power output of the laser to be evaluated:

$$P = \frac{1}{2} N c \hbar v T_r \pi r^2 \quad (26)$$

The factor 1/2 takes into account that half the photons are travelling away from the output mirror of transmission $T_r = (1-r_2)$, c is the velocity of light, $\hbar v$ the energy of the lasing photons of 1.868×10^{-20} J. Experimentally it was found that the output beam had a radius of 0.3 cm corresponding to a Gaussian profile in a 4 cm radius tube, (ref. 13) and for $T_r = 0.05$,

$$P = 3.97 \times 10^{-12} N \text{ (W)} \quad (27)$$

Plots of power output vs. total pressure p (torr) for different black body temperatures are given in Figure 3. The gases were in the ratio CO_2 16%, He 4%, Ar 80°. The output power rises with black body temperature, but as p increases, the power falls. The effect is due to the R_1 term in the equations; on making $R_1 = 0$ the output power rose with increasing pressure.

The variation of output power with black body temperature at a fixed total pressure of 7 torr, but with the same gas ratios, is shown in Figure 4. A linear rise is observed.

The gas temperature of T_g can be altered by assuming different wall temperatures T_w . Assuming a gas mixture as before of 7 torr (16% CO_2 , 4% He, 80° Ar) and a black body temperature of 1450K, then the power output vs. T_g is plotted in Figure 5. It shows that an increase in gas

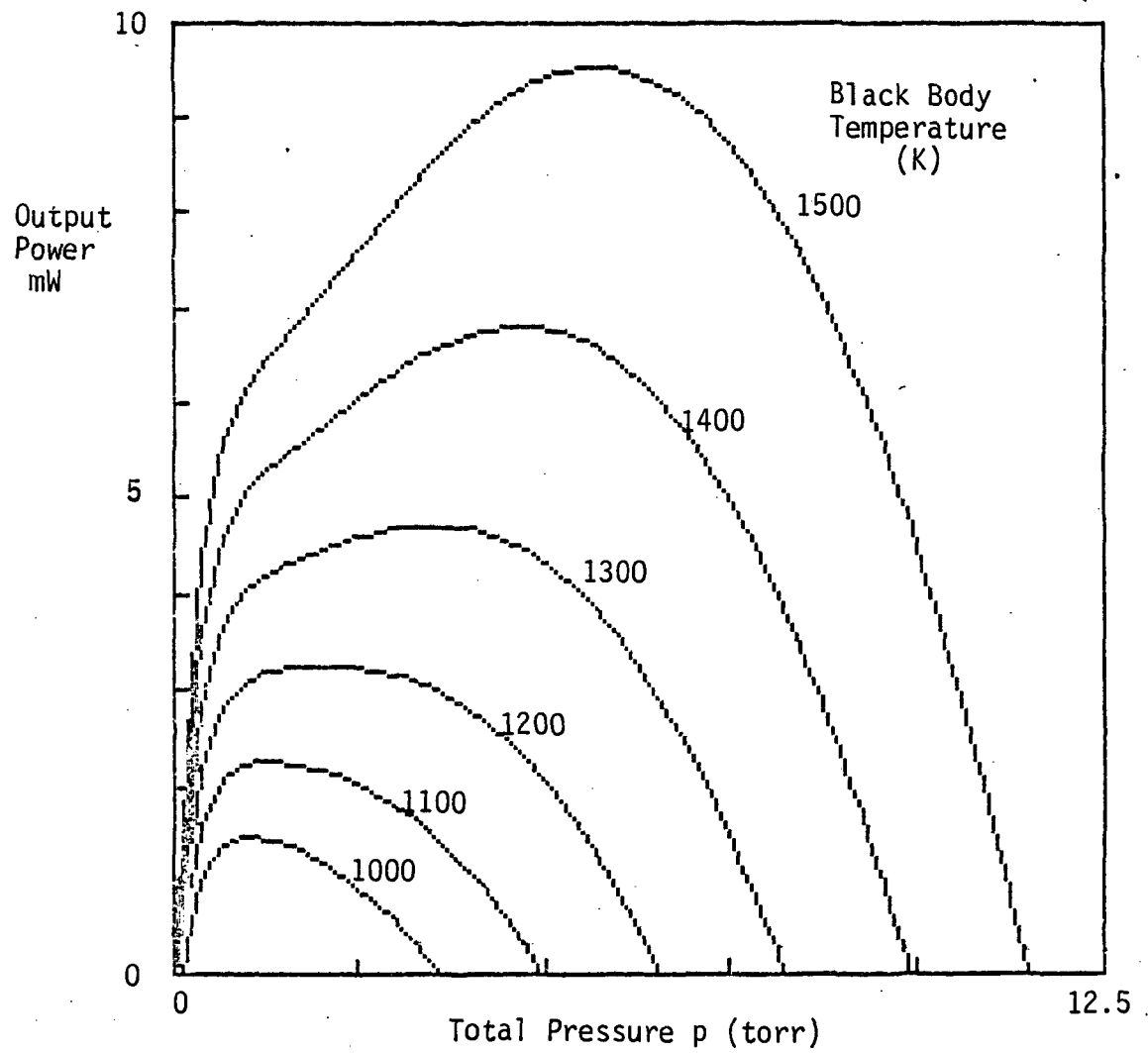


Figure 3. Power output of black body pumped laser vs total pressure for various black body temperatures. The gases were CO₂-16%, He-4%, Ar-80%. The wall temperature was 340K.

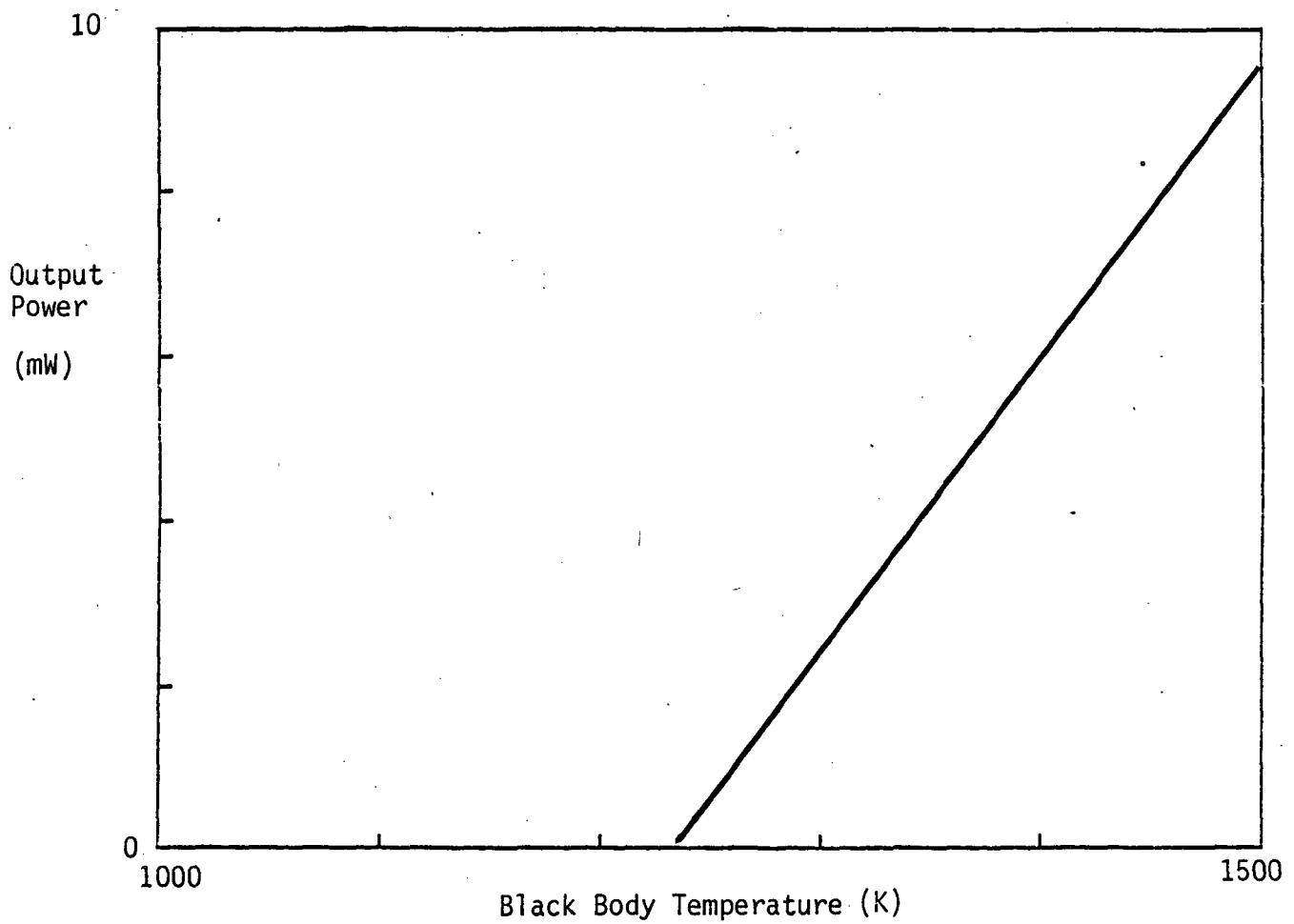


Figure 4: Power output vs black body temperature. Total pressure = 7 torr, 16% CO₂, 4% He, 80% Ar, wall temperature 340K.

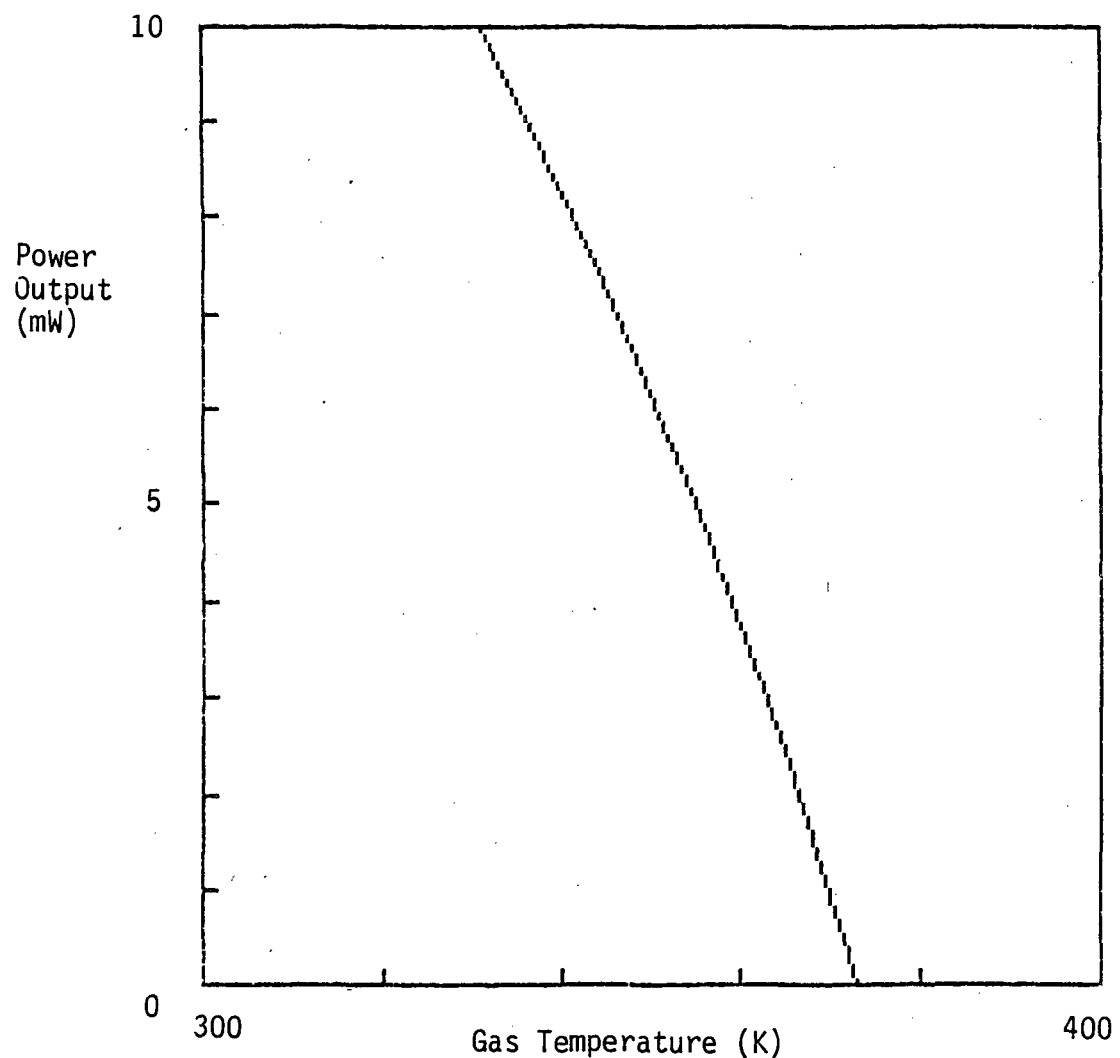


Figure 5. Plot of power output vs gas temperature, 7 torr 16% CO₂, 4% He, 80% Ar, black body temperature 1450K.

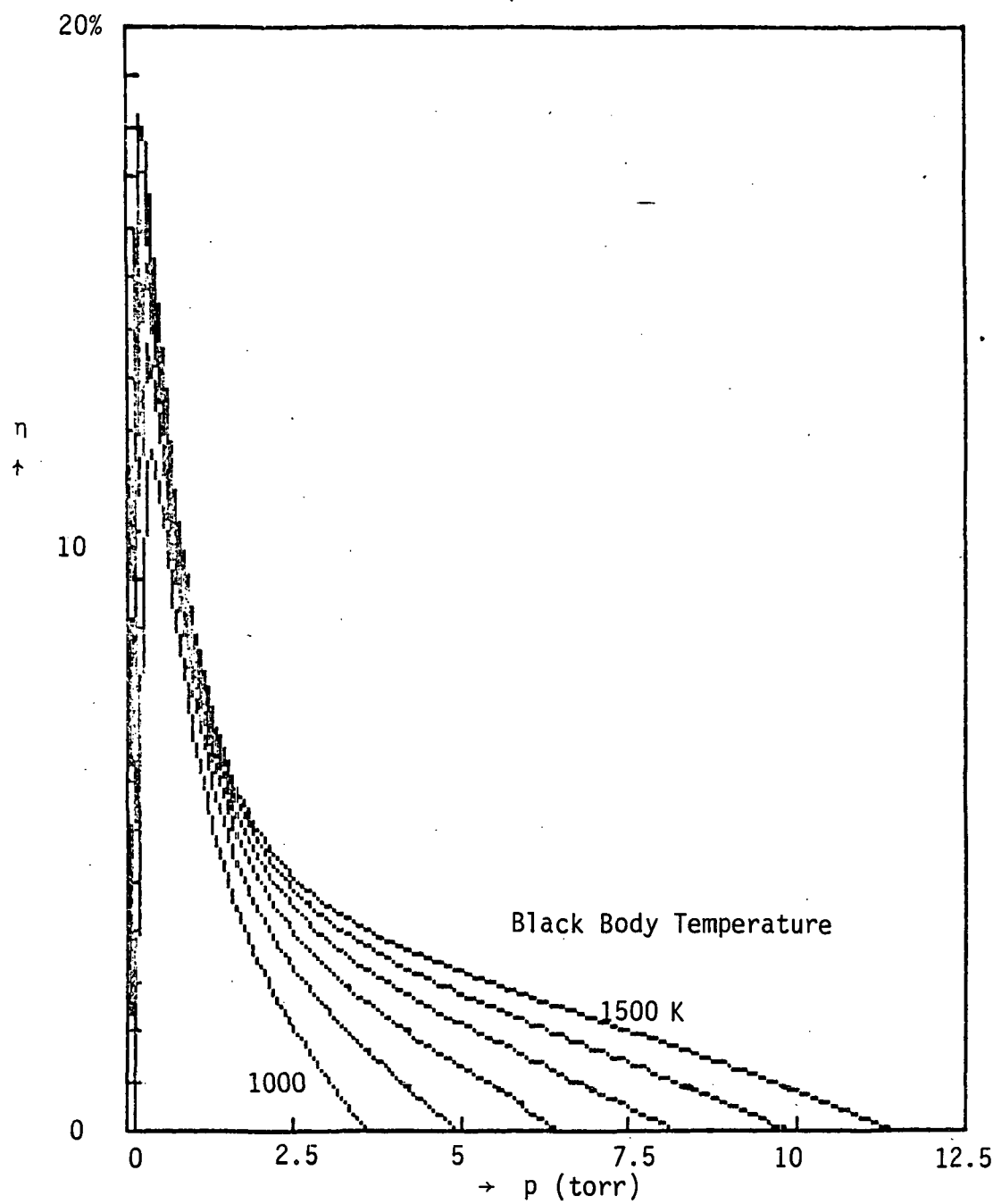


Figure 6. Efficiency (as defined in equation 29) of the black body pumped laser vs total pressure p for various black body temperatures. The gases are CO_2 16%, He 4% and Ar 80%.

temperature greatly reduces the output power indicating that cooling of the medium is essential.

4.2 Efficiency

The input power P_{in} is the power absorbed by the laser:

$$P_{in} = E(\lambda) d\lambda 2\pi r L (1 - \exp(-(CO_2)\sigma_a 2r)) \quad (28)$$

and the efficiency η is defined here as output power/the power absorbed from the black body radiation:

$$\eta = P/P_{in} \quad (29)$$

(It should be noted that the black body pumped laser has other "efficiencies" besides η , however, these are not considered here.)

Using equation 29 to define the efficiency, Figure 6 shows plots of η vs. p for different black body temperatures. There seem to be high efficiencies at very low pressures where the output power is small. In the regime around 7 torr where experimentally the highest output powers were observed, the efficiency is only a few percent.

CONCLUSIONS

The results here depend critically on the values of the rate coefficients in Table 1. They are insensitive to K_4 , K_5 , K_6 , but are very dependent on K_9 , K_{11} and K_{13} . The most sensitive parameter seems to be K_{11} where a change of a few percent altered the output power by several times. Also τ_D was a sensitive parameter.

Unfortunately, the rate coefficient for R_1 was not known. The values

chosen indicate that about one collision in 10^5 of two ground state atoms resulted in the creation of one CO₂(100) which does not seem unreasonable.

Figures 3, 4, and 5 show reasonable qualitative agreement with experimental measurements (ref. 1). However, it did not seem possible to get agreement with experimental measurements of power output vs. total pressure (ref. 12), at a black body temperature of 1450K where the ratios CO₂:He:Ar were varied. In view of this, these results must be treated with caution, and must be regarded as preliminary.

ACKNOWLEDGEMENTS

The authors acknowledge useful discussions with Dr. W. E. Meador and Dr. J. W. Wilson of NASA Langley Research Center, and with Ms. R. J. Insuik of the University of Washington.

REFERENCES

1. R.J. Insuik and W.H. Christiansen, IEEE J. Quantum Electronics QE-20, 622, (1984).
2. J.F. Coneybear, "The Use of Lasers for the Transmission of Power. Radiation Energy Conversion in Space," K.H. Billman, ed., Program astronaut Aeronaut 61, 279, 1979.
3. W.L. Harries and J.W. Wilson, Space Solar Power Review 2, 367, 1981.
4. W.L. Harries and W.E. Meador, Space Solar Power Review 4, No. 3, 189, 1983.
5. A. Javan and M. Guerra, NASA Contractor Report H3428 under contract NAS1-14688, p. 13, 1981.
6. Alvon Engel, "Electric Plasmas and their Uses," Taylor & Francis Ltd., p. 37, 1983.
7. Alvon Engel, "Ionized Gases," Oxford University Press, p. 140, 1964.
8. R.L. Taylor and S. Bitterman, Rev. Mod. Phys. 41, 26, 1969.
9. J.A. Blauer and G.R. Nickerson, AIAA 4th Fluid and Plasma Dynamics Conference, Palo Alto, CA, June 17-19, 1974, Paper 74-536.
10. J.A. Blauer and G.R. Nickerson, Technical Report AFRPL-TR-73-57 for Nov. 72-May 1983.
11. P.A. Lewis and D.W. Trainor "Survey of Relaxational Data for O₂, N₂, NO H₂, CO, HF, HCl, CO₂ and H₂O, Avco Everett Research Lab Inc., Contract No. F04701-73-C-0284. Nov. 1974.
12. S.A. Munji and W.H. Christiansen, App. Optics 12, 993, (1973).
13. R. J. Insuik, Private communication.

APPENDIX

Diffusion of CO₂ When Mixed with He and Ar

The mean free paths of molecules in their own gas at 1 torr for CO₂, He and Ar are 2.7x10⁻³ cm, 13.1x10⁻³ cm and 4.6x10⁻³ cm, respectively (ref. 7). These values give the cross sectional diameters, and it is then assumed that for a collision between unlike molecules that the cross section diameter is the arithmetic mean of the individual diameters. Adding the collision frequencies of CO₂-CO₂, CO₂-He, CO₂-Ar, the total collision frequency ν for CO₂ is:

$$\nu = 2.37 \times 10^{-11} (\text{CO}_2) \left(1 + 1.79 \frac{\text{He}}{\text{CO}_2} + 2.54 \frac{\text{Ar}}{\text{CO}_2} \right) \sqrt{T} \quad (\text{A1})$$

The diffusion coefficient D is then

$$D = \frac{1}{3} \frac{v_r^2}{\nu} = 1.928 \times 10^6 T / \nu$$

where $v_r = 2405 \sqrt{T}$ is the random velocity of CO₂.